Available online at www.sciencedirect.com
ScienceDirect
Ceramics International 38 (2012) 1019–1025
CERAMICS INTERNATIONAL
www.elsevier.com/locate/ceramint

Phase evolution and microwave dielectric properties of $MgO–B_2O_3–SiO_2$–based glass–ceramics

Urban Došler *, Marjeta Maček Kržmanc, Danilo Suvorov

"Jožef Stefan" Institute, Jamova 39, 1000 Ljubljana, Slovenia

Received 12 May 2011; received in revised form 8 August 2011; accepted 11 August 2011
Available online 19 August 2011

Abstract

The densification and crystallization behaviors of $MgO–B_2O_3–SiO_2$ (MBS) glass with various amounts of TiO_2 additions (0–10 wt.%) were investigated by means of thermal analysis, X-ray powder diffraction and scanning electron microscopy. A microwave dielectric characterization was performed in order to evaluate the suitability of MBS glass–ceramics as a low-permittivity dielectric substrate. The densification of the MBS glass started below 700 °C. The main crystalline phases of $Mg_2B_2O_5$ and $MgSiO_3$ appeared at 800 and 950 °C, respectively. The $Mg_3TiB_2O_8$ and $TiB_{0.024}O_2$ phases additionally crystallized in TiO_2-added MBS glass–ceramics at 1000 °C. The permittivity increased from 6.1 in pure MBS glass to 6.9 in MBS glass with 10 wt.% of TiO_2. The addition of TiO_2 enhanced the crystallization and consequently increased the Qxf-values of the MBS glass (11 300 GHz) up to 16 500 GHz. The improvement of the Qxf-values became the most evident at 1050 °C. Dense MBS glass–ceramics sintered at $850 \leq T \leq 950$ °C exhibited Qxf-values of 5000–8000 GHz (at ~12 GHz), which are comparable with the values of $CaO–B_2O_3–SiO_2$-based glass–ceramics.

Keywords: D. Glass–ceramics; Crystallization; Microwave dielectric properties; Nucleating agent

1. Introduction

In the past 20 years wireless communications have become one of the fastest-growing segments in the consumer-electronics industry. The widespread usage of several different wireless systems has required the development of materials and process technologies that can provide the rapid production of low-cost, lightweight, small, multifunctional and highly reliable devices. Low-temperature co-fired ceramics (LTCC) technology is one of the most promising approaches to realize these goals. A typical LTCC module consist of several layers of substrate material with buried passive components, such as capacitors, inductors, resistors, resonators and filters, that are interconnected with 3D stripline circuitry. The simultaneous firing of the electrodes (Ag, Cu or Au) and the ceramic substrate material requires a low sintering temperature with electrodes that are compatible with ceramics. In addition to these basic requirements, the LTCC substrate materials should exhibit a low permittivity ($\varepsilon_r < 8$) to reduce the signal propagation delay, low dielectric losses (tan δ), i.e., a high quality factor ($Q = 1/\tan\delta$) [1–3], and a stable temperature coefficient of resonant frequency (τ_f).

The majority of low-permittivity, high-Q materials sinter at much higher temperatures than that required by LTCC technology. This is the reason why the methods that have been developed for the preparation of low-permittivity LTCC substrates include the addition of a low-melting glass. The commercially available LTCC substrates fall into two major categories: glass + ceramics (multiphase ceramics) [4–6] and glass–ceramics (crystallizable glass) [7–9]. In the former method, low-softening glass is mixed with filler ceramics where the low-softening glass reduces the sintering temperature and increases the densification. In the latter method the crystalline phases are formed during firing. Complete densification and sufficient crystallization are prerequisites for good mechanical properties and high Q-values of the substrate materials. Due to the higher Q-values the glass–ceramic systems seem to be more promising for applications in LTCC modules than glass and ceramic mixtures. The glass + ceramic representatives are the borosilicate glass + alumina system of Fujitsu [10] and the lead

* Corresponding author. Tel.: +386 1 477 3991; fax: +386 1 251 9385.
E-mail address: urban.dosler@ijs.si (U. Došler).

0272-8842/$36.00
doi:10.1016/j.ceramint.2011.08.025

borosilicate glass + alumina system of Dupont [11]. Typical glass–ceramic systems have been developed by IBM [12] (crystallizable cordierite), Motorola [13] (crystallizable anorthite) and Ferro [14] (crystallizable calcium silicates and calcium borate).

Glass–ceramics based on the $CaO–B_2O_3–SiO_2$ system have been widely investigated by several researchers. These glass–ceramics are promising LTCC substrate materials because of their low dielectric losses, low firing temperature and compatibility with several metal electrodes [15–18]. The commercial representative from the $CaO–B_2O_3–SiO_2$ system is the Ferro A6 LTCC material [14]. To the best of our knowledge, the crystallization of $MgO–B_2O_3–SiO_2$ (MBS) glass and the dielectric properties of the corresponding glass–ceramics have not been reported so far. Taking into account several low-permittivity and high-Q compounds (Mg_2SiO_4 [19], $MgSiO_3$ [20], $Mg_3B_2O_6$ [21] and $Mg_2B_2O_5$ [22]) that crystallize in the $MgO–B_2O_3–SiO_2$ system, the glass–ceramics from this system are expected to exhibit promising dielectric properties.

In this paper we introduce new $MgO–B_2O_3–SiO_2$-based (MBS) glass–ceramics with the composition 35 wt.% MgO–43 wt.% B_2O_3–22 wt.% SiO_2. The main purpose of the work was to study the sintering and crystallization behavior with respect to the microwave dielectric properties. The influence of the TiO_2 nucleating agent on the crystallization and microwave dielectric properties of these glass–ceramics was also examined and discussed.

2. Experimental procedure

A glass composition that contained 43 wt.% MgO, 35 wt.% B_2O_3 and 22 wt.% SiO_2, was selected according to preliminary studies and the $MgO–B_2O_3–SiO_2$ phase diagram [23]. The initial reagent-grade raw materials of MgO (Sigma Aldrich, 98%), B_2O_3 (Alfa Aesar, 99.98%), and SiO_2 (Alfa Aesar, 99.8%) were dried and weighed in the ratio described above. After 1 h of mixing and homogenization with zirconia balls (d = 5 mm) in a turbula mill the powder mixture was melted in a platinum crucible for 30 min at 1350 °C in air and quenched by pouring onto a graphite plate to minimize the possibility of crystallization. The glass was then crushed with a vibration mill and in order to ensure complete homogenization of the glass the whole melting procedure was repeated. This melting regime was found to be sufficient to yield homogeneous, transparent and colourless quenched glass frit with no visible non-melted remains and crystalline inclusions. The last of these was confirmed by X-ray analyses. The glass powder for the sintering was prepared by 2-h milling in acetone with Y-stabilized ZrO_2 balls (d = 3 mm) in a planetary mill. The glass powders were uniaxially pressed at about 100 MPa to obtain green compacts with a diameter of 12 mm and a thickness of around 4 mm. The controlled crystallization of the glass was carried out in air in the temperature range from 800 to 1050 °C at a heating rate of 10 °C/min for a duration of 5 h in the tube furnace. The MBS glass with the addition of the TiO_2 nucleating agent was prepared using a similar procedure. TiO_2, in the amount of 1–10 wt.%, was homogenized with the MgO, B_2O_3 and SiO_2 powders before melting at 1500 °C. The sintering and melting behavior of the glass–ceramics was examined with a heating microscope (EM 201, Hesse instruments, Osterode, Germany) at a constant heating rate of 10 °C/min. The differential thermal analyses (DTA) of the glass powders were performed on a Jupiter 449 simultaneous thermal analysis (STA) instrument using the alumina crucible. The crystalline phases formed during annealing were identified by powder X-ray diffraction (XRD) analysis using a D4 Endeavor (Bruker AXS, Karlsruhe, Germany) X-ray diffractometer with Cu Kα radiation (1.5406 Å). The chemical etching of the polished samples was performed in an acid solution containing HNO_3 and HF. The microstructural studies of the etched samples were conducted with a field-emission scanning electron microscope (FE-SEM), JSM-7600, JEOL, Tokyo, coupled with an energy-dispersive X-ray spectrometer (EDX) and software (Series II X-ray microanalyzer, Tracor Northern, Middleton, WI). The densities of the sintered glass–ceramic specimens as a function of sintering temperature were evaluated by the Archimedes liquid-displacement method using an analytical balance and acetone as the reference liquid. The radio-frequency (RF) dielectric measurements were performed at 1 MHz on Au-plated disk capacitors using a high-precision LCR meter (Agilent 4284 A). The permittivities measured in the RF frequency range were used for the identification of the corresponding $TE_{01\delta}$ mode in the microwave (MW) frequency range (∼12 GHz). The MW dielectric properties were characterized using the dielectric resonator method, described by Krupka et al. [24], using a network analyzer (HP 8719C).

3. Results and discussion

3.1. Crystallization, sintering and microstructure of $MgO–B_2O_3–SiO_2$ (MBS) glass–ceramics

The typical events that occurred during the transformation from glass to glass–ceramics were clearly visible in the DTA curve of the MBS glass in Fig. 1. The inflection at 660 °C was attributed to the glass-transition temperature, while the exothermic peak at 870 °C was ascribed to the crystallization

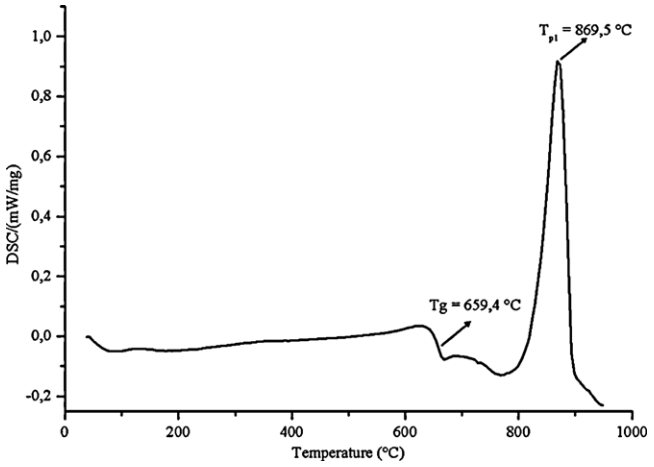

Fig. 1. Differential thermal analysis (DTA) curve of MBS glass powder.

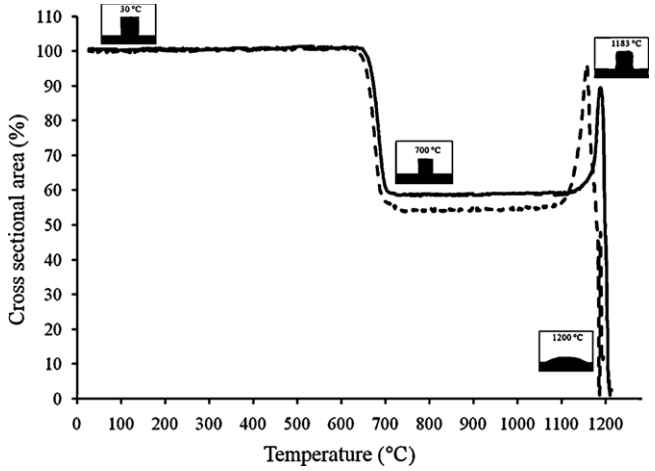

Fig. 2. Sintering profile of the milled MBS glass powder (—) and MBS glass powder with 10 wt.% of TiO_2 (- - - -).

of $Mg_2B_2O_5$. The formation of $Mg_2B_2O_5$ was confirmed with the XRD analysis of the powder after the DTA experiment and also with the HT-XRD measurements of the MBS glass at the temperature of the DTA peak.

The sintering kinetics was examined with heating-microscope measurements (Fig. 2). Since the method monitors the change of the pellet's silhouette during heating, the shrinkage and enlargement of the pellet results in a decrease and an increase of its cross-sectional area, respectively. A comparison between the DTA and heating-microscope measurements showed that the intense shrinkage started above the glass-transition temperature (Figs. 1 and 2). In the temperature range where the crystallization occurred, no shrinkage was observed (Figs. 1 and 2). This could be expected since it is known that the formation of the crystalline phase at an early stage retards the densification [25]. The increase of the cross-sectional area of the pellet above 1100 °C indicates the beginning of the melting (Fig. 2). The densification behavior of the glass powder did not change significantly with the addition of the TiO_2 nucleating agent (Fig. 2). Thus, the same annealing conditions as for pure MBS glass–ceramics were applied also for the preparation of the glass–ceramics with the addition of TiO_2 (1–10 wt.%).

The phase evolution during the isothermal annealing at various temperatures from 800 to 1050 °C was followed by powder XRD (Fig. 3). No crystallization occurred at temperatures below 800 °C. Magnesium borate ($Mg_2B_2O_5$), which has a triclinic crystal modification with the space group S.G. $P\bar{1}$, was the main crystalline phase in the XRD pattern of the glass–ceramic powder annealed at 800 °C. The broad diffraction lines indicate the small size of the crystallites. The sharpening and increase of intensity of the majority of the diffraction lines indicates the growth of the $Mg_2B_2O_5$ crystallites and the increase of the $Mg_2B_2O_5$ phase content with an increase in the temperature. At annealing temperatures higher than 950 °C the $MgSiO_3$ phase appeared. The proximity of the $Mg_2B_2O_5$ and $MgSiO_3$ diffraction lines caused an apparent broadening of some of the diffraction lines, especially in the 2θ range from 34 to 36°.

The TiO_2 nucleating agent was added in order to promote the crystallization of the MBS glass. TiO_2 is one of the most commonly used nucleating agents since it has a twofold effect on crystallization. Firstly, TiO_2 promotes a metastable liquid–liquid phase separation, which acts as the starting point for the internal crystallization of the glass [26]. Secondly, TiO_2 can form small primary crystalline precipitates, which are additional heterogeneous nucleation sites for the crystallization [27]. In silica-containing glasses TiO_2 is easily miscible in the glassy networks at high temperatures, but induces a phase separation during the cooling of the melt [28].

The small additions of TiO_2 (1 wt.%) did not change the phase constitution of the MBS glass. The $Mg_2B_2O_5$ predominantly crystallizes at 800–950 °C, whereas the $MgSiO_3$

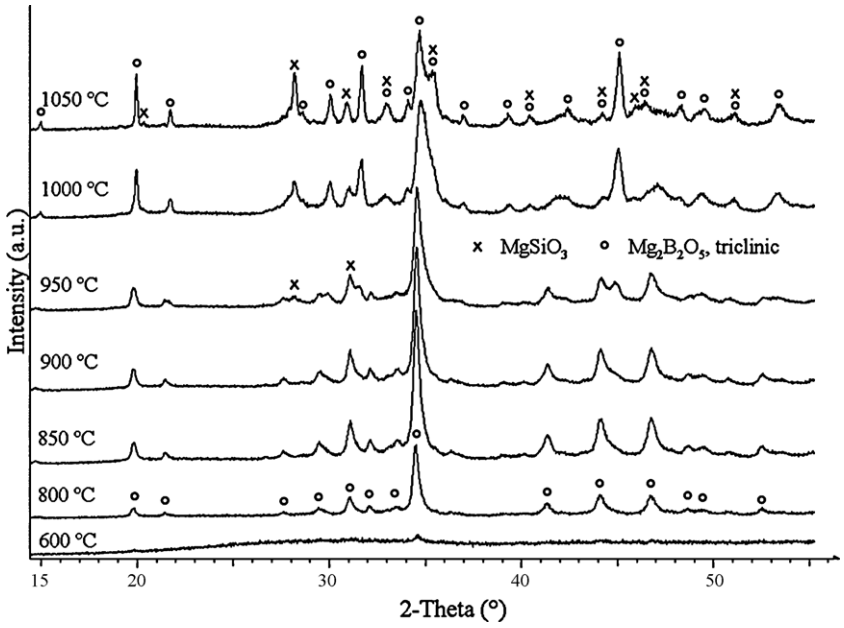

Fig. 3. Powder XRD patterns of MBS glass–ceramics after annealing (10 h) at denoted temperatures.

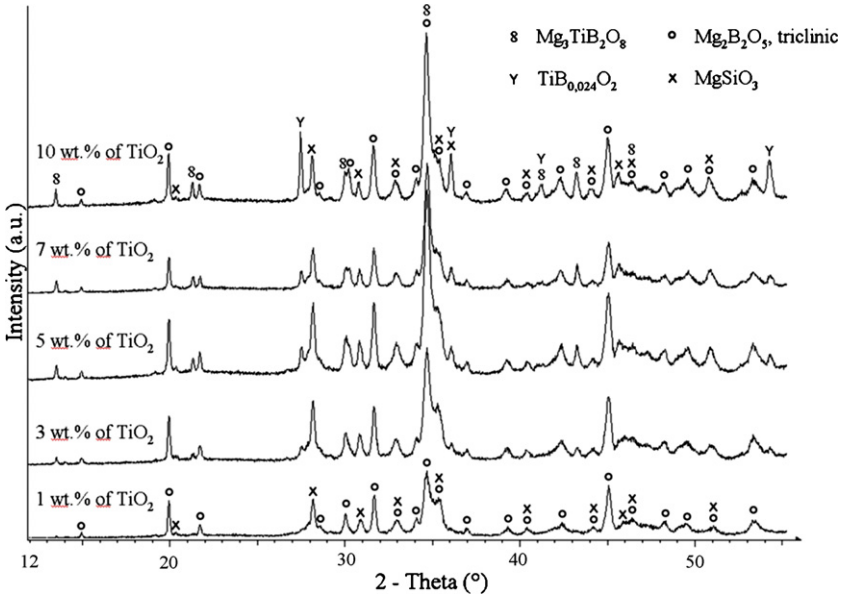

Fig. 4. Powder XRD patterns of the MBS glass–ceramics with various amounts of TiO_2, annealed at 1050 °C for 10 h.

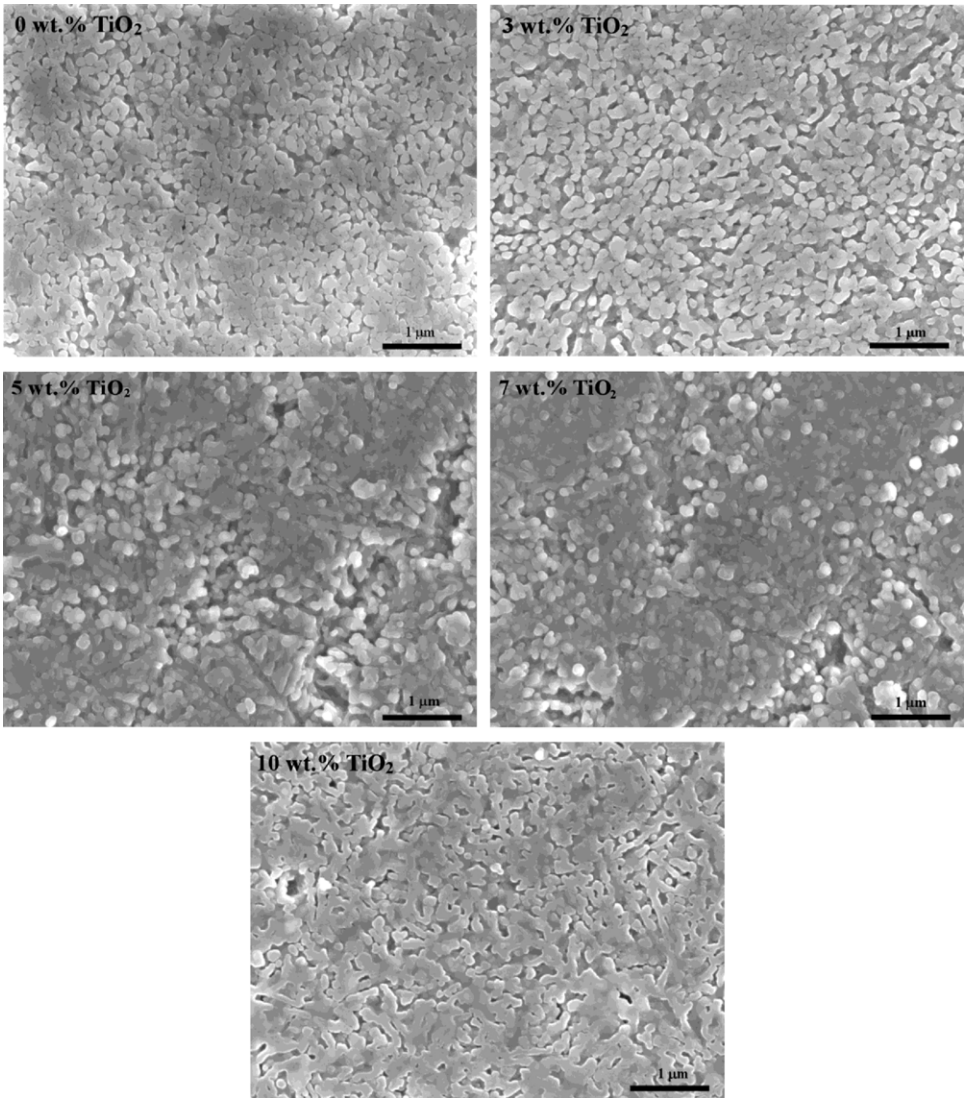

Fig. 5. SEM micrographs of MBS glass–ceramics with various amounts of TiO_2 sintered at 1000 °C.

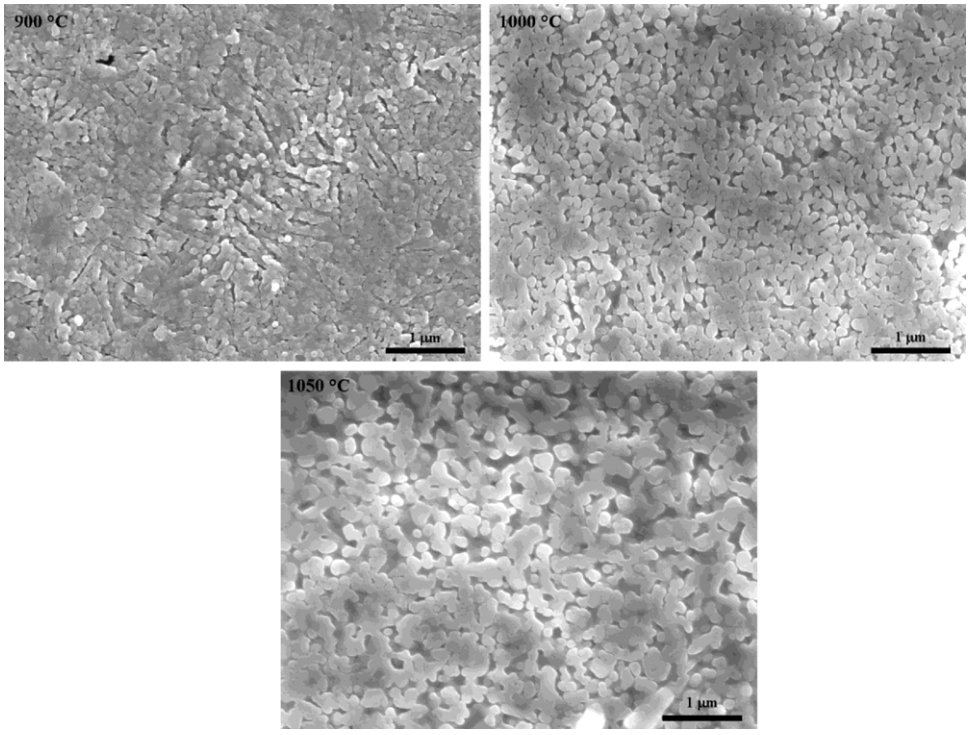

Fig. 6. SEM micrographs of pure MBS glass–ceramics sintered at 900 °C and 1050 °C.

appeared at $T \geq 950$ °C. With an increasing amount of TiO_2, additional crystalline phases started to form. Diffraction lines of warwickite ($Mg_3TiB_2O_6$) (PDF 75-1192) [29] and boron-doped rutile ($TiB_{0.024}O_2$) (PDF 87-0921) [29] were identified at $T > 1000$ °C. The peaks of warwickite and rutile doped with boron were identified for the samples with TiO_2 contents greater than 1 wt.%. The intensity of the crystal phase peaks increases with the TiO_2 addition. The XRD patterns of the MBS glass–ceramic with various amounts of added TiO_2 annealed at 1050 °C for 10 h are shown in Fig. 4. The intensity of the diffraction lines evidently increases with the amount of TiO_2, indicating an increase of the crystalline-phase content. Due to the prolonged heat treatment (10 h) at selected temperatures the phase constitution of the isothermally annealed glass–ceramics differed from that obtained after the single DTA run, where only the $Mg_2B_2O_5$ crystallized, irrespective of the TiO_2 content. The addition of TiO_2 in an amount of 1–10 wt.% was found to have no significant effect on the grain size of the glass–ceramics (Fig. 5). The glass–ceramics sintered at 1000 °C exhibited a grain size in the range 70–190 nm. The increase in the sintering temperature from 900 to 1050 °C resulted in an increase of the grain size from 50 to more than 200 nm, respectively (Fig. 6).

3.2. Microwave dielectric characterization

In accordance with the densification behavior observed with the heating microscope, the highest density of the MBS glass was already achieved at 800 °C. With a further increase in temperature the density slightly decreased (Fig. 7), which is the main reason for a minor decrease of the permittivity (Fig. 8). A larger decline of the density together with the permittivity was observed for the MBS glass with 10 wt.% of TiO_2 sintered at 1050 °C. We believe the reason for such a drop in the values could be attributed to the melting and thus to the faster growth of the grains and pores. The pores grow by an Ostwald-ripening mechanism due to the higher solubility of smaller pores in the matrix than that of the larger pores. However, as a consequence of differing solubilities, the larger pores grow at the expense of the small pores. The permittivity could also alter due to the variation in the crystalline-phase content, which changed with the temperature and the time. Due to the similar low permittivities of the MBS glass, $Mg_2B_2O_5$ ($\varepsilon = 6.6$) [22] and $MgSiO_3$ ($\varepsilon = 6.7$) [20], the small differences in the phase composition are not believed to significantly influence the permittivity. The addition of TiO_2 caused an increase in the

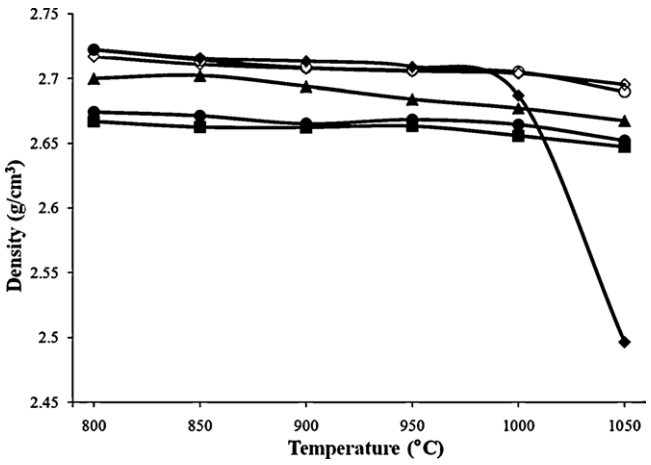

Fig. 7. Density of MBS glass ceramics with various amounts of TiO_2 as a function of sintering temperature: (■) without TiO_2, (●) 1 wt.%, (▲) 3 wt.%, (◇) 5 wt.%, (○) 7 wt.%, and (◆) 10 wt.% of TiO_2.

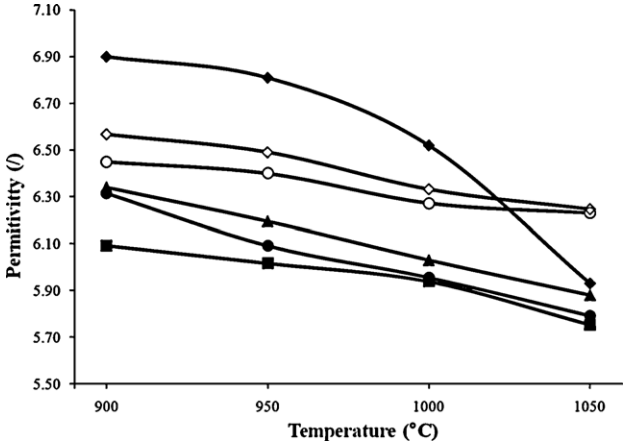

Fig. 8. Permittivity of MBS glass–ceramics with various amounts of TiO_2 as a function of sintering temperature: (■) without TiO_2, (●) 1 wt.%, (▲) 3 wt.%, (◇) 5 wt.%, (○) 7 wt.%, and (◆) 10 wt.% of TiO_2.

density and the permittivity of the MBS glass (Figs. 7 and 8). The permittivity changed from 6.9 to 6.1 for the MBS glass with and without TiO_2, respectively. The drop of the permittivity with decrease of the TiO_2 content was expected because of the higher dielectric polarizability of titanium compared to the other constituting elements in the glass. TiO_2 exhibits a permittivity of 105 and Qxf-values of 40 000 GHz [30]. The contribution of the $Mg_3TiB_2O_8$ phase to the permittivity of the TiO_2-added glass could not be exactly evaluated because its dielectric properties, to the best of our knowledge, have not been reported so far. Like with pure MBS glass, the TiO_2-added glass also displayed a slight decrease of permittivity with temperature, which coincided with the lowering of the density. In contrast to the permittivity, the Qxf-values increased with the sintering temperature and with the amount of TiO_2 (Fig. 9). The increase of the crystalline-phase content was recognized as the main reason for the improvement of the Qxf-values. The highest Qxf-value above 16 500 GHz was measured for the MBS glass with 10 wt.% of TiO_2, sintered at 1050 °C. The annealing at such a high temperature is excessive for the LTCC sintering with Ag, Cu and Au electrodes. Furthermore, the MBS glasses sintered at 1050 °C exhibited a density that is lower than the maximum density. However, the sintering of the MBS glass at 850–950 °C led to dense glass–ceramics with Qxf-values of 5000–8000 GHz, which are comparable with the values reported for $CaO–B_2O_3–SiO_2$ glass–ceramics [25,31,32] Many attempts were made to improve the densification behavior and the dielectric properties of MBS glass–ceramics. Among them, a two-stage sintering approach was applied to increase the densification of the MBS glass–ceramics. In the two-stage sintering process the pressed pellet of the glass was initially heated to a temperature slightly above T_g, and annealed for 10 h to enhance the densification and then heated to the final temperature, where it was annealed for an additional 10 h. Since we found that such an annealing procedure did not influence the density and final dielectric properties, single-stage sintering, as described in the experimental section, was used for the preparation of the MBS glass–ceramics. With the nucleation of the MBS glass at the temperature of the maximum nucleation rate (688–700 °C), which was determined in the separate experiments, we tried to increase the crystalline phase content and consequently to improve the Qxf-values. However, no significant improvement in the Qxf-values was achieved.

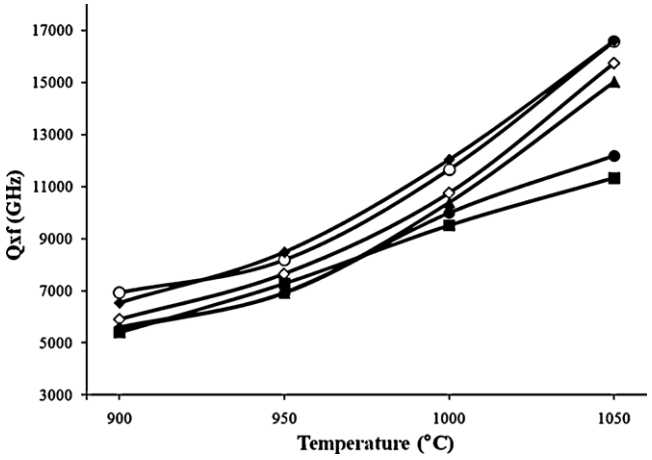

Fig. 9. Qxf-values of MBS glass–ceramics with various amounts of TiO_2 as a function of sintering temperature: (■) without TiO_2, (●) 1 wt.%, (▲) 3 wt.%, (◇) 5 wt.%, (○) 7 wt.%, and (◆) 10 wt.% of TiO_2.

4. Conclusions

In this study, $MgO–B_2O_3–SiO_2$-based (MBS) glass–ceramics were prepared by the controlled crystallization of the glass with the composition $MgO:B_2O_3:SiO_2$ = 43 wt.%:35 wt.%:22 wt.% and with TiO_2 additions of 0–10 wt.%. The glass–ceramics that consist of two main phases, namely $Mg_2B_2O_5$ and $MgSiO_3$, were characterized in terms of their crystallization behavior and microwave dielectric properties. The phase compositions of the glass–ceramics strongly depended on the annealing temperature. $Mg_2B_2O_5$ started to crystallize at $T \approx 800$ °C, while $MgSiO_3$ appeared at 950 °C. The $Mg_3TiB_2O_8$ and $TiB_{0.024}O_2$ phases were additionally found in the TiO_2-added MBS glass–ceramics annealed at 1000–1050 °C. Both the permittivity and Qxf values increased with the TiO_2 content. The improvement of the Qxf-values was attributed to the enhanced crystallization. The highest Qxf value of 16 500 GHz was measured for the MBS glass–ceramics with 10 wt.% of TiO_2 sintered at 1050 °C. The MBS-based glass–ceramics sintered in the range from 850 to 950 °C exhibited somewhat lower Qxf-values of 5000–8000 GHz and ε = 6.1–6.9. However, these values are comparable to the values of similar glass–ceramic systems such as $CaO–B_2O_3–SiO_2$.

References

[1] C.L. Lo, J.G. Duh, B.S. Chiou, W.H. Lee, Low-temperature sintering and microwave dielectric properties of anorthite-based glass–ceramics, J. Am. Ceram. Soc. 85 (9) (2002) 2230–2235.
[2] R.J. Cava, Dielectric materials for applications in microwave communications, J. Mater. Chem. 11 (2001) 54–62.

[3] M. Udovič, D. Suvorov, Sintering and dielectric characterization of pseudoternary compounds from the Bi_2O_3–TiO_2–TeO_2 system, J. Am. Ceram. Soc. 90 (8) (2007) 2404–2408.
[4] T. Takada, S.F. Wang, S. Yoshikawa, S.J. Jang, R.E. Newnham, Effect of glass additions on BaO–TiO_2–WO_3 microwave ceramics, J. Am. Ceram. Soc. 77 (7) (1994) 1909–1916.
[5] S.X. Dai, R.F. Huang, D.L. Wilcox, Use of titanates to achieve a temperature-stable low-temperature cofired ceramic dielectric for wireless applications, J. Am. Ceram. Soc. 85 (4) (2002) 828–832.
[6] O. Dernovsek, A. Naeini, G. Preu, W. Wersing, M. Eberstein, W.A. Schiller, LTCC glass–ceramic composites for microwave application, J. Eur. Ceram. Soc. 21 (2001) 1693–1697.
[7] R.R. Tummala, Ceramic and glass–ceramic packaging in the 1990, J. Am. Ceram. Soc. 74 (5) (1991) 895–908.
[8] J.H. Jean, Y.C. Fang, S.X. Dai, D.L. Wilcox, Devitrification kinetics and mechanism of K_2O–CaO–SrO–BaO–B_2O_3–SiO_2, J. Am. Ceram. Soc. 84 (6) (2001) 1354–1360.
[9] H.K. Zhu, M. Liu, H.Q. Zhou, L.Q. Li, A. Lv, Study on properties of CaO–B_2O_3–SiO_2 system glass–ceramic, Mater. Res. Bull. 42 (2007) 1137–1144.
[10] Y. Imanaka, N. Kamehara, Influence of shrinkage mismatch between copper and ceramics on dimensional control of the multilayer ceramic circuit board, J. Ceram. Soc. Jpn. 100 (4) (1992) 560–564.
[11] C.R. Chang, J.H. Jean, Crystallization kinetics and mechanism of low dielectric, low-temperature, cofirable CaO–B_2O_3–SiO_2 glass–ceramics, J. Am. Ceram. Soc. 82 (7) (1991) 1725–1732.
[12] A.H. Kumar, P.W. McMillan, R.R. Tummala, Glass–ceramic structures and sintered multilayered substrates thereof with circuit patterns of gold, silver, or copper, US Patent 4,301,324 (1981).
[13] S.J. Bethke, R.A. Miesem, W.W. Chiou, R.G. Pastor, Ceramic composition, US Patent 5,821,181 (1998).
[14] M.T. Sebastian, H. Jantunen, Low-loss dielectric materials for LTCC applications: a review, Int. Mater. Rev. 53 (2) (2008) 57–90.
[15] S.H. Wang, H.P. Zhou, Densification and dielectric properties of CaO–B_2O_3–SiO_2 system glass ceramics, Mater. Sci. Eng. B 99 (2003) 597–600.
[16] J.H. Jean, C.R. Chang, C.D. Lei, Sintering of a crystallizable CaO–B_2O_3–SiO_2 glass with silver, J. Am. Ceram. Soc. 87 (7) (2004) 1244–1249.
[17] H.K. Zhu, H.Q. Zhou, M. Liu, P.F. Wei, G. Ning, Low temperature sintering and properties of CaO–B_2O_3–SiO_2 system glass ceramics for LTCC applications, J. Alloys Compd. 482 (2009) 272–275.
[18] S.F. Wang, C.C. Chiang, Y.R. Wang, Y.F. Hsu, Effects of additives on the densification and microwave dielectric properties of binary CaO–B_2O_3–SiO_2 glass, Jpn. J. Appl. Phys. 49 (2010) 021101.
[19] H. Ohsato, Research and development of microwave dielectric ceramics for wireless communications, J. Ceram. Soc. Jpn. 113 (11) (2005) 703–711.
[20] M.E. Song, J.S. Kim, M.R. Joung, S. Nahm, Y.S. Kim, J.H. Paik, B.H. Choi, Synthesis and microwave dielectric properties of $MgSiO_3$ ceramics, J. Am. Ceram. Soc. 91 (8) (2008) 2747–2750.
[21] U. Došler, M.M. Kržmanc, B. Jančar, D. Suvorov, A high-Q microwave dielectric material based on $Mg_3B_2O_6$, J. Am. Ceram. Soc. 93 (11) (2010) 3788–3792.
[22] U. Dosler, M.M. Kržmanc, D. Suvorov, The synthesis and microwave dielectric properties of $Mg_3B_2O_6$ and $Mg_2B_2O_5$ ceramics, J. Eur. Ceram. Soc. 30 (2010) 413–418.
[23] H.J. Kuzel, Untersuchung des dreistoffsystems MgO–B_2O_3–SiO_2, Neues Jahrb. Miner. 100 (3) (1963) 322–338.
[24] J. Krupka, K. Derzakowski, B. Riddle, J.B. Jarvis, A dielectric resonator for measurements of complex permittivity of low loss dielectric materials as a function of temperature, Meas. Sci. Technol. 9 (1998) 1751–1756.
[25] C.C. Chiang, S.F. Wang, Y.R. Wang, W.C.J. Wei, Densification and microwave dielectric properties of CaO–B_2O_3–SiO_2 system glass–ceramics, Ceram. Int. 34 (2008) 599–604.
[26] W. Höland, P. Wange, K. Naumann, J. Vogel, G. Carl, C. Jana, W.J. Götz, Control of phase formation processes in glass–ceramics for medicine and technology, J. Non-Cryst. Solids 129 (1991) 152–162.
[27] G. Carl, T. Höche, B. Voigt, Crystallisation behaviour of a MgO–Al_2O_3–SiO_2–TiO_2–ZrO_2 glass, Phys. Chem. Glasses 43C (2002) 256–258.
[28] S.R. Lacerda, J.M. Oliveira, R.N. Correia, M.H.V. Fernandes, TiO_2-induced phase separation and crystallization in SiO_2–3CaO·P_2O_5–MgO glass, J. Non-Cryst. Solids 221 (1997) 255–260.
[29] PCPDFWIN Version 2.3, JCPDS-International Center for Diffraction Data, June 2001.
[30] S.H. Yoon, D.W. Kim, S.Y. Cho, K.S. Hong, Phase analysis and microwave dielectric properties of LTCC TiO_2 with glass system, J. Eur. Ceram. Soc. 23 (2003) 2549–2552.
[31] S.F. Wang, Y.R. Wang, Y.F. Hsu, C.C. Chiang, Densification and microwave dielectric behaviors of CaO–B_2O_3–SiO_2 glass–ceramics prepared from a binary glass composite, J. Alloys Compd. 498 (2010) 211–216.
[32] H.K. Zhu, H.Q. Zhou, M. Liu, P.F. Wei, G.J. Xu, G. Ning, Microstructure and microwave dielectric characteristics of CaO–B_2O_3–SiO_2 glass ceramics, J. Mater. Sci.: Mater. Electron. 20 (11) (2009) 1135–1139.